

Understanding the Self-Healing Hydrophobic Recovery of High-Voltage Insulators

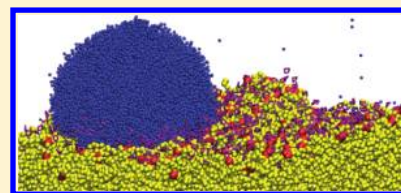
Philip T. Shemella,[†] Teodoro Laino,^{*,†} Oliver Fritz,[‡] and Alessandro Curioni[†]

[†]IBM Research—Zurich, Säumerstrasse 4, 8803 Rüschlikon, Switzerland

[‡]ABB Switzerland Ltd., Corporate Research, 5405 Baden-Dättwil, Switzerland

S Supporting Information

ABSTRACT: Amorphous siloxane polymers are designed to have high dielectric strength for use as high-voltage insulation materials. Surface hydrophobicity is essential and can be impaired by environmental, electrical, or mechanical factors, leading to leakage currents due to dielectric breakdown. Self-recovery is possible and is generally observed over a period of several hours. Using large-scale, all-atom molecular dynamics simulations, the surface wetting of water droplets on the polymer surface is simulated for various surface conditions, including oxidation and coating with small molecules, to understand the driving forces of the recovery process at the atomistic level, which is of primary importance for the developments of novel materials. In this work, we shed light onto the self-recovery mechanism and propose the use of low-molecular-weight (LMW) siloxane to accelerate the recovery of hydrophobicity.



■ INTRODUCTION

Siloxane materials, composed of a silicon–oxygen backbone and hydrocarbon side chains, are found in a wide range of products and materials. The applications of synthetic, amorphous siloxane polymers are widespread; to name just a few: as lubricants,¹ for microfluidics,^{2,3} for biomedical devices⁴ and drug delivery,⁵ for sensor technology,⁶ as thermal⁷ and electric insulators,^{8,9} and even as a skin-care excipient^{10,11} or food additive.^{12,13} At the core of these applications is polydimethylsiloxane (PDMS), a relatively inert but extremely adaptable material. The ubiquity of PDMS and the myriad of applications are due to its tailorable properties, which can be designed a priori for a specific application. Contributing parameters to material properties are polymer length, side chain composition, and mixture ratios between different molecules. In addition, chemical cross-linking between molecular groups can be used to increase the rigidity of the material.

In this work, we focus on amorphous PDMS mixtures that are used as high-voltage insulators. These materials are exposed to the environment and are subject to mechanical stress and corona discharges, all of which can impair the dielectric strength.^{14–16} In fact, with dielectric breakdown, the surface hydrophobicity is damaged, and leakage currents can result.^{16–19} The material itself can undergo a self-recovery process: when PDMS surfaces are exposed to oxidative conditions, such as in presence of a corona discharge in air, hydrophobicity is lost, and between 8 and 50 days are needed for the hydrophobic properties of the unexposed surface²⁰ to recover. The repair mechanism, unknown as of today, is thought to be based on either surface dipole rearrangement¹⁹ or the diffusion of small molecules to the surface.^{16,21–23} It can be completely inhibited if desired.²⁴ Although several research efforts have characterized the essential conditions for hydro-

phobic repair,^{20,24} a fundamental understanding of the underlying mechanism is still missing at the atomic and molecular levels. Using large-scale molecular dynamics simulations on an amorphous surface system with various conditions of surface damage, we aim to shed light on the mechanisms of hydrophobic self-recovery. Because of their small size and accelerated diffusion,²² low-molecular-weight (LMW) siloxanes, produced by depolymerization reactions after UV exposure, electrical discharges, or heating, are thought to contribute to the self-healing hydrophobic recovery.

As already outlined above, after an oxidative event, charged groups at the surface destroy the material's water-repellent properties. To probe surface hydrophobicity, contact angles of water droplets on the polymer surface are measured. Experimentally, the contact angle has been shown to transition from highly hydrophobic ($\sim 120^\circ$), to hydrophobic ($>90^\circ$), and then hydrophilic ($<90^\circ$) with complete surface wetting.^{15,17,18,20} Schneemilch and Quirke simulated the wettability of the PDMS surface and found a contact angle of 125° for an untreated surface, which decreased to 75° for a fully hydroxylated surface.²⁵ Ismail et al. simulated the surface tension and contact angle of the hydrophobic surface.²⁶

In this article, we study the interface between a water droplet and the PDMS surface with all-atom molecular dynamics simulations for various surface oxidation conditions. We find that, because of their ring geometry, small cyclomethicone compounds (i.e. LMW siloxanes) have a unique interaction with polar and charged molecules while simultaneously preserving their hydrophobic property. On the basis of our calculations, we propose a rationale for accelerating and

Received: January 24, 2012

Revised: May 22, 2012

Published: May 24, 2012

improving the repair mechanism of surface hydrophobicity after an oxidative event.

METHODS

Model System. We use a model system that has been previously studied, both as a bulk system²⁷ and as a surface system.²⁸ The surface consisted of a slab with a thickness of ~22 nm, with the periodic directions having a box length of 23.3 nm.

We base our model system on a mixture of small and large siloxane molecules,²⁹ which is representative of the commercial product Sylgard-184 (Dow Corning), frequently studied because of its industrial importance.^{17,18,20} Molecular components are based on PDMS, which has a repeating polymeric unit of Si–O with two methyl groups and is given in Table 1.

Table 1. Size Comparison for Molecular Groups Shows Orders of Magnitude Differences in Molecular Weight and Chain Length^a

	mol wt (g/mol)	no. of atoms	degree of polymerization (DP)
PDMS	72562.3	9789	978
PMHS	1966.2	237	32
D8	592.8	80	8
D4	296.4	40	4

^aIn addition to size differences, D4 and D8 are nonlinear, cyclic molecules.

The larger molecule, pure PDMS with vinyl termination, has a degree of polymerization (DP) of 978, corresponding to a molecular mass of 72 562.3 g/mol/molecule. Sixty-seven PDMS molecules were used, resulting in ~95% of the mass of the system. Considerably smaller than the PDMS molecules used, 132 “cross-linker” molecules (~5 w/w %) were included (DP = 32) on the basis of polymethylhydrosiloxane (PMHS). Cross-linker molecules had trimethyl ($-(\text{CH}_3)_3$) termination, and the molecular mass of each molecule was 1966.2 g/mol. The “bare” surface of the model system consisted of PDMS and PMHS (cross-linker) molecules described above.

In addition to these linear molecules, LMW cyclomethicone molecules were included. These small ring molecules are the byproduct of depolymerization reactions²² and have the same composition as PDMS, but with a ring geometry. Because of their small size, even compared with the cross-linker molecules, these LMW ring molecules may play a key role in the self-recovery mechanism. For this reason, we have calculated the diffusion, binding, and the effect D4 (molecular mass of 296.4 g/mol) and D8 (molecular mass of 592.8 g/mol), consisting of four and eight polymeric units, respectively, have on the hydrophobicity. Figure 1 shows a size comparison for all molecular components, together with a pictorial view of the full system under investigation.

Force Field. For the polymer system, a force field based on the work of Smith et al.³⁰ was used. Covalent bonds were treated with either harmonic or class II bonding terms.^{31–34} In addition to the standard class II force field, a correction for the discontinuity of energy at the Si–O–Si linearization point was implemented^{25,30} to represent accurately the physical behavior of the polymer backbone. Full force field data is provided separately in the Supporting Information.

Nonbonded interactions were cut off at 10.0 Å, and 1–2 and 1–3 atom pairs were not computed (interactions between 1 and 4 atom pairs were reduced by half). Lennard-Jones energies were calculated on the basis of the $1/r^6 + 1/r^{12}$ form and were fit to the Buckingham potential.³⁰ Coulombic interactions were treated with the $1/r$ form. A time step of 2.0 fs was used for a system without water molecules, whereas in all other cases, a time step of 1.0 fs was used. Molecular dynamics simulations were performed with a Langevin thermostat having a coupling constant of 10.0 ps. The SHAKE algorithm³⁵ was used to constrain covalent bonds involving hydrogens. All calculations have been performed with the LAMMPS code^{36,37} on the IBM Blue Gene supercomputer family.³⁸

Atomic charges were based on the work of Smith et al.,³⁰ with several modifications: vinyl carbon atoms that terminate the PDMS molecules had a charge of $-0.205e$; nonterminal Si atoms on the PMHS (cross-linker) molecules had a charge of $+0.804e$, and H atoms bonded to those Si had a charge of

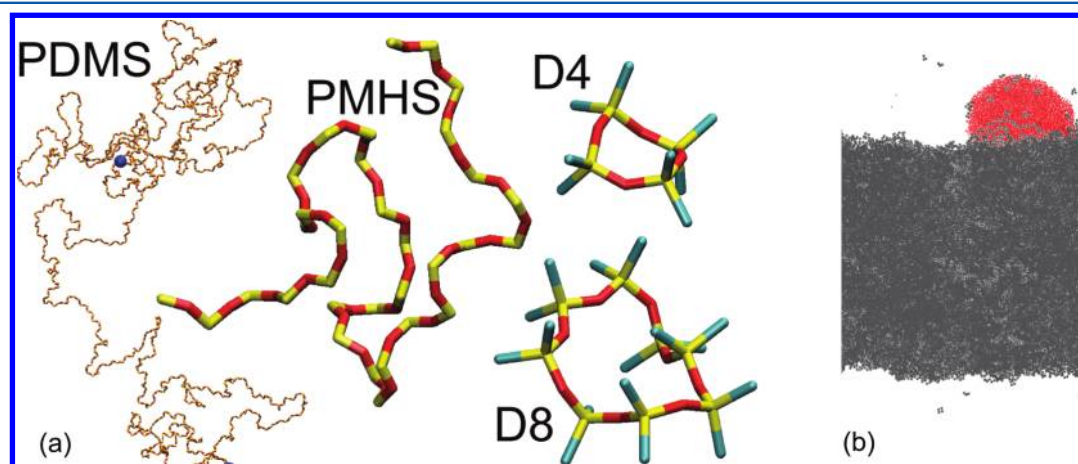


Figure 1. (a) Size comparison of molecular species (not to scale). PDMS has a degree of polymerization (DP) of 978 monomeric units with vinyl ($-\text{CH}=\text{CH}_2$) termination (9789 atoms, MW ~72 500 g/mol). The cross-linker molecule, PMHS, has a DP of 32 with trimethyl termination (237 atoms, MW ~1966). D4 is a dimethyl siloxane ring of 4 backbone units (40 atoms) and a molecular weight of 296.6 g/mol. D8 has 8 backbone units, 80 atoms, and a molecular weight of 593.2 g/mol. The periodic directions have a box length of 23.3 nm, and the nonperiodic direction is 30.0 nm, or 35.0 nm for simulations with a water droplet. (b) Pictorial view of the full system under investigation (in gray, the polymeric blend, including PDMS, PMHS and D4; in red, the water droplet).

−0.198e. For nonoxidized systems, each molecule was charge-neutral, as was the total system. For oxidized systems, a methyl group was replaced with a carboxylate (−COO[−]), and a negative charge was distributed over the partial atomic charges of the carboxylate's oxygens. Sodium atoms (Na⁺), used as counterions to mimic the formation of oxidized ionic pairs, had a charge of +1.0e and Lennard-Jones parameters based on Aqvist.³⁹

The short-range parametrized form of the standard four-site model for water, TIP4P, was used for the droplet⁴⁰ with a 10 Å cutoff. The droplet was placed near the surface at several locations and allowed to equilibrate on the surface (>1 ns of equilibration). Mixing parameters between the siloxane molecules and TIP4P water are given in Table 2 and are nearly equivalent to those used by Ismail et al. for SPC/E water molecules.²⁶

Table 2. Mixing of Nonbonded Interactions between TIP4P Water and Siloxane Molecules^a

nonbonded pair	ϵ_{ij} (kcal/mol)	σ_{ij} (Å)
Si–O _W	0.1958	3.4915
O–O _W	0.1767	3.0018
C–O _W	0.1233	3.2958
H–O _W	0.0393	3.0791

^aNo mixing terms were calculated for H_W from TIP4P water molecules.

Contact Angle Calculations. To probe the hydrophobic properties of the surface, we equilibrated a water droplet with a radius of ~50 Å (17 580 molecules) on the surface, then calculated the macroscopic three-phase contact angle by means of the isochoric density-binning method,^{41,42} averaging the density profiles over more than 1 ns of simulation time. The isochoric density-binning method^{41,42} is based on the cylindrical binning of water droplet slices from the top of the droplet to the surface of the material. The radial density was calculated for each cylindrical bin every 5 ps, from the center of the droplet outward, and the equimolar dividing surface was calculated by fitting the density to

$$\rho(z) = \rho_0 \tanh\left(\frac{2(z - z_e)}{d}\right) \quad (1)$$

where ρ_0 is the bulk density of the liquid water, d is a measure of the interfacial thickness, and z_e is the height of the equimolar surface. For each fitted density profile, z_e was fit to a circle. The angle between the surface and the tangent to the circle is the contact angle: values larger than 90° correspond to a hydrophobic surface, and values smaller than 90° to a hydrophilic surface.

RESULTS

The bulk system and the surface structure have been prepared as already reported in our previous works.^{27,28} It is worth recalling here that the surface structure consists of methyl groups that are nonrandomly aligned, as shown by order parameters analysis^{26,28,43} as well as by experimental measurements.⁴⁴ The magnitude of the structural order parameter (S) for either methyl carbons or backbone silicons is defined as

$$S(z) = \frac{1}{2} \langle 3 \cos^2 \theta - 1 \rangle \quad (2)$$

where θ is the angle between the normal and the molecular vector. Full details, including the analysis of the present surface, have been reported elsewhere.²⁸ For completeness, here we recap that our calculations showed a large number of methyl groups at the surface pointing outward, an orientation that produces surface hydrophobicity. Because the number of methyl groups exposed at the surface is relevant for understanding the nature of the charge-oxidized damage, we report in Table 3 the average number of methyl groups per

Table 3. Average Concentration of Methyl Groups within 3.0 Å of the Local Surface, per Squared nm^a

	PMHS	PDMS	D4
bare	0.42	4.92	
low [D4]	0.36	5.04	0.48
high [D4]	0.30	3.66	1.81

^aMost methyl groups available for oxidation are part of the large PDMS molecules, decreasing their mobility considerably when compared with cross-linkers or D4.

square nanometer, calculated for several simulated surface structures, together with the average values. Low and high concentrations of D4 molecules corresponded to 121 and 484 molecules, respectively, and are described later for contact angle calculations. The large abundance of PDMS methyl groups, as compared with PHMS, the latter being only 5% of the system mass, reveals that the PDMS moiety is the one most likely to be damaged by corona discharges. Within PDMS, the methyl groups are the most probable candidates for oxidation. In fact, the other plausible PDMS oxidation site, that is, the vinyl terminal groups, may contribute only with few scattered superficial charges, a number too small to impair hydrophobicity. Therefore, the PDMS methyls groups, exposed to the air, provide an upper estimate of the maximum number of carbon atoms available for oxidation.

To predict the surface/bulk affinity of the LMW molecules, we computed the binding energies for D4 and D8 molecules, both at the surface and embedded in the material, at 500 K. The average binding energies for a D4 molecule in the center of the material was -15.51 ± 0.13 kcal/mol, and at the surface, -15.27 ± 0.30 kcal/mol (the confidence level represents the standard error of the mean). For a D8 molecule, the binding energies were -32.47 ± 0.23 kcal/mol in the center and -31.98 ± 0.48 kcal/mol at the surface. We also calculated the average internal energy for the D4 and D8 molecules. In going from the center to the surface, the average internal energy of the D4 molecule decreased by ~0.5 kcal/mol, whereas that of D8 decreased by ~0.8 kcal/mol. Comparing the energetic properties of D4 and D8, their binding is determined only by their size (number of methyl groups). At the same time, for D4 and D8, the molecular strain experienced in the bulk material, as opposed to that when freely moving on the surface, was overall similar, within sampling errors.

Diffusion constants were calculated for the D4 and D8 molecules embedded in the center of the slab. At 500 K, the average diffusion for D4 was 2×10^{-6} cm²/s, and for D8, it was 6×10^{-7} cm²/s. In distance, this corresponds to 1 mm in 8 h for D4 and in 28 h for D8. For the larger D8, diffusion estimates at 500 K correspond to the diffusion of the cross-linker from both this calculation and our previous bulk study.²⁷ For this reason and because D4 and D8 exhibit similar binding

properties, the subsequent set of calculations includes large sets of only D4 molecules.

Identical in chemical composition to PDMS, D4 has no terminal groups and exhibits geometrical rigidity due to constrained torsion angles. Despite having the same methyl groups that contribute to surface hydrophobicity, the oxygen atoms were observed to form hydrogen bonds with hydrogen atoms of the water molecules. This attractive, nonbonded interaction was not observed for linear polymeric molecules (PDMS, PMHS). Linear molecules have a flexible backbone that allows the oxygen to be shielded from water molecules by methyl groups, preventing the formation of a hydrogen bond. Figure 2 shows the radial distribution functions between the

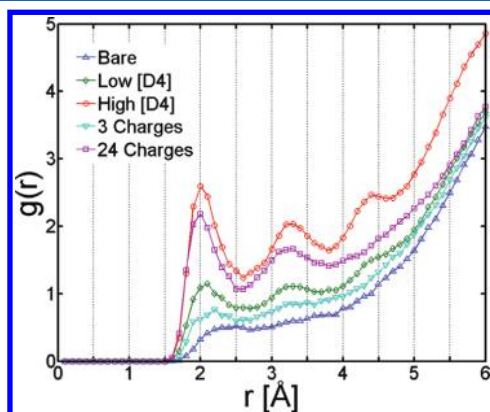


Figure 2. Radial distribution functions between polymeric oxygen atoms and hydrogen atoms belonging to water molecules ($H_{\text{Water}} - O_{\text{Polymer}}$). The peak around 2.0 Å for systems containing D4 correlates to the hydrogen bond formed between the hydrogen atom of a water molecule and the oxygen atom of the D4 molecule, which, because of its unique ring structure, is more exposed for this type of interaction.

hydrogen of water molecules and the oxygen of the polymeric materials. For the bare surface, there is no peak at 2.0 Å, the distance for a hydrogen bond. For systems with several oxidized groups, a peak at 2.0 Å begins to form, which is due to those charged groups interacting with water molecules. When D4 is added to the bare system, a similar peak is observed for oxygen atoms belonging to D4 molecules. These peaks indicate an affinity for water similar to the system with charged end groups (see Figure 2).

Hydrogen bonds between D4 and water are local and involve only one water molecule per oxygen. Moreover, no long-range network of water on the surface was observed. For this reason, the attractive interaction between D4 and water does not damage surface hydrophobicity. If the same type of interaction D4 experiences with water is also present with oxidized groups, D4-like molecules could be used to preserve a hydrophobic surface by shielding charged groups from the water droplet.

To verify this hypothesis, we simulated PDMS surface wetting by equilibrating a water droplet on the surface of the polymeric material and calculating the contact angle. Two charge schemes were used: first, localized charges near the interface with the droplet; and second, a quasi-random scheme with nonlocalized charges. On the basis of estimations from experiment,⁴⁵ two concentrations of D4 were considered for contact-angle simulations. For the low concentration, a total of 121 D4 molecules (0.7 w/w %) was deposited on the upper and the lower surfaces, corresponding to a concentration of 0.11 molecules/nm². For the high concentration, comprising

484 D4 molecules (2.7 w/w %), the concentration was equal to 0.44 molecules/nm². Two concentrations were chosen for surface coating to give estimates for sparse or partial D4 coverage. The higher concentration allowed for more interactions between D4-type molecules and a thicker and more continuous coating of LMW molecules. Even with the largest concentration of D4 molecules, the majority of methyl groups exposed at the surface were part of the long PDMS chains.

Contact Angles. The contact angle for the untreated, bare surface was 123°, in very good agreement with the experimental value of 125°. Multiple simulation trajectories for the water droplet at various locations on the surface indicated that the measured error in the contact angle was smaller than the differences calculated for various surface conditions (i.e., with an average error of ~1°). Moreover, we found that order parameters for methyl groups under the water droplet reflect a more ordered structure than those for methyl groups not under the water droplet, in agreement with experimental observations.⁴⁴ Figure 3A shows a side view of the water droplet on a hydrophobic surface (bare).

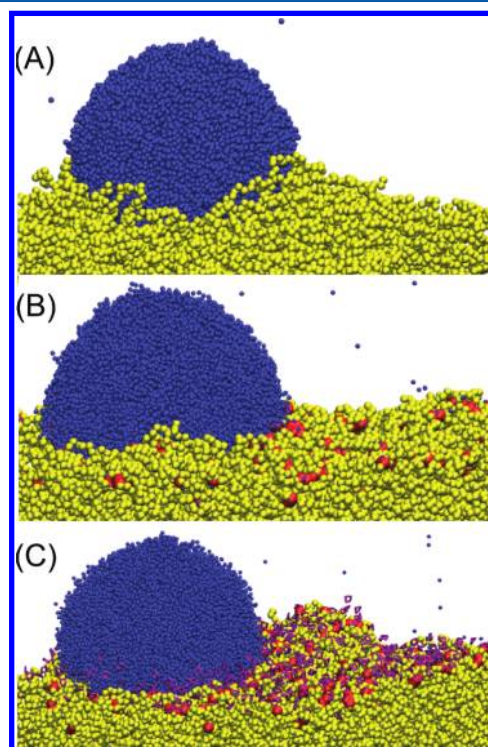


Figure 3. (A) The bare surface is extremely hydrophobic, as shown by a side view of the water droplet on the surface. (B) With the inclusion of oxidized methyl groups ($-\text{COO}^-$) and Na^+ counterions, the surface becomes hydrophilic, as shown by a contact angle less than 90°. (C) When D4 molecules are added to the system with oxidation and counterions, surface hydrophobicity is recovered. Without the counterions, this recovery is not possible.

For the low and high concentrations of D4 molecules, the contact angles were 125° and 123°, respectively. When the methyl groups under the water droplet were oxidized, the contact angle decreased to 118°. With random positioning of oxidized groups, there is no systematic way to quantify the hydrophilic effect, and for 3–5 negative charges, the contact angle remained similar. For 24 charges beneath the droplet

(0.04 charges/nm²), the contact angle decreased to 113°. This local region of oxidation did not create a hydrophilic surface, which corresponds to a contact angle of <90°; this is expected because there are no oxidized sites distributed across the entire surface, a necessary condition for wetting. Unless methyl groups from all molecular groups are candidates for oxidation, there will not be a sufficient number of exposed groups to contribute to a hydrophilic surface.

To understand widespread and nonlocal damage, we oxidized a high concentration of methyl groups at the surface. These methyls were chosen on the basis of their proximity to the local surface and were quasirandom because they were chosen to be at least 8 Å away from another negative charge. Maximum oxidation included 400 charged groups on the upper surface, corresponding to 0.73 charges/nm². The contact angle for this system decreased to ~85°, corresponding to a hydrophilic surface. Wetting was observed to proceed until there was a gap between surface charges.

Next, D4 molecules were deposited on top of the 400 oxidized groups, and water was equilibrated for contact-angle measurements. Although the D4 shielded the droplet from the negative charges, the contact angle recovered only up to a value of ~96°. This minor recovery of the hydrophobicity is not surprising because D4 oxygens do not have any attractive interaction with negative charges and the shielding of their interactions with water is only partial. In fact, many oxidized groups still remained exposed and in contact with the water droplet.

Nonetheless, in any realistic situation, the formation of either neutral oxidized groups or, alternatively, oxidized ionic pairs occurs predominantly. Therefore, we considered a system with 200 negatively charged methyl groups (0.36 negative charges/nm²) and 200 Na⁺ counterions (0.36 positive charges/nm²), shown in Figure 3B. The upper surface was overall charge-neutral but heavily polarized, and the contact angle was ~80°. Under these conditions, the surface of the insulating material would be hydrophilic, and dielectric strength could be impaired.

To recover surface hydrophobicity, a high concentration of D4 molecules was deposited onto the hydrophilic surface that already contained 200 oxidized groups and 200 Na⁺ counterions. After equilibration of the water droplet, the D4 coating played an active role in shielding the droplet from the charges (see Figure 3C). The average concentration of D4 within 5.0 Å of the water droplet increased to 1.91 molecules/nm² from the mean value of 0.88 molecules/nm². The unique ring structure of D4 enabled an attractive interaction between D4 molecules and both positively charged Na⁺ ions as well as with hydrogen atoms of water molecules. The increased concentration of D4 near the droplet contributed to the recovery of a hydrophobic contact angle of ~102°. This value, larger than the 80° computed without the presence of D4 molecules, unequivocally proves the recovery of a hydrophobic surface due to LMW ring molecules.

Recovery Mechanism. The proposed mechanism for the self-recovery of surface hydrophobicity can be outlined as follows: Upon action of external factors favoring strong oxidative conditions, such as corona discharge in the presence of high humidity content, the PDMS undergoes molecular degradation processes either by the oxidation of methyl groups or by formation of silicate chains (as a result of the decomposition of PDMS backbone). This degradation process is responsible for the temporary loss of dielectric strength, as

well as for the shift of the surface wettability from hydrophobic to hydrophilic.

On the basis of our simulations, we have identified the driving force of the self-healing with the small, cyclic molecules (D4 and D8), naturally present in small quantities in commercial PDMS, due to the chemical equilibrium between longer polymeric chains and small cyclic moieties. The small, cyclic molecules can be considered crucial for hydrophobic recovery because they can diffuse quickly through the material, and at the same time, while having hydrophobic properties, they *solvate* the defects induced by the surface oxidation, thanks to their rigid molecular structure. Therefore, the migration of D4 and D8 molecules on the damaged polymer surface results in a coverage with a thin layer of hydrophobic material. While D4 and D8 *solvate* the charged degradation products by means of chemical interactions, they also shield these groups from any environmental water, restoring the material hydrophobicity. This process is what we identify as the main recovery channel.

We also envisage that upon surface coverage (by D4 and D8), additional longer time-scale processes may take place, tending to move the degraded surface, although stabilized by the interaction with D4 and D8, to the inner part of the PDMS matrix, with a complete renewal of the material surface.

CONCLUSIONS

One cause of the reduced dielectric strength of high-voltage PDMS-based insulating materials is their exposure to corona discharges, which leads to superficial damages with subsequent loss of hydrophobicity. In this article, we have identified the small, PDMS-based ring molecules as possible candidates to promote the self-recovery process, thanks to their unique interaction with polar groups, while still contributing to a hydrophobic surface and to their diffusion time scales, faster than the diffusion of either PDMS or PHMS. On the basis of our calculations, these small ring molecules can be added to shield damaged surface oxidation sites that would otherwise cause wetting of the surface. In this way, the self-healing hydrophobic recovery is accelerated, due to the increased diffusivity of D4 compared to PDMS and PHMS, quickly restoring the material's integrity.

ASSOCIATED CONTENT

Supporting Information

Additional information as noted in text. This material is available free of charge via the Internet at <http://pubs.acs.org>.

AUTHOR INFORMATION

Corresponding Author

*E-mail: teo@zurich.ibm.com.

Notes

The authors declare no competing financial interest.

REFERENCES

- (1) Bongaerts, J. H. H.; Fourtouni, K.; Stokes, J. R. *Tribol. Int.* **2007**, *40*, 1531–1542.
- (2) McDonald, J. C.; Duffy, D. C.; Anderson, J. R.; Chiu, D. T.; Wu, H.; Schueller, O. J. A.; Whitesides, G. M. *Electrophoresis* **2000**, *21*, 27–40.
- (3) Dendukuri, D.; Panda, P.; Haghgooei, R.; Kim, J. M.; Hatton, T. A.; Doyle, P. S. *Macromolecules* **2008**, *41*, 8547–8556.
- (4) Abbasi, F.; Mirzadeh, H.; Katbab, A. A. *Polym. Int.* **2001**, *50*, 1279–1287.

- (5) Rösler, A.; Vandermeulen, G. W. M.; Klok, H. A. *Adv. Drug Delivery Rev.* **2001**, *53*, 95–108.
- (6) Lötters, J. C.; Olthuis, W.; Veltink, P. H.; Bergveld, P. J. *Micromech. Microeng.* **1997**, *7*, 145–147.
- (7) Loo, Y. L.; Willett, R. L.; Baldwin, K. W.; Rogers, J. A. *J. Am. Chem. Soc.* **2002**, *124*, 7654–7655.
- (8) Lacour, S. P.; Wagner, S.; Huang, Z.; Suo, Z. *Appl. Phys. Lett.* **2003**, *82*, 2404.
- (9) Loo, Y. L.; Someya, T.; Baldwin, K. W.; Bao, Z.; Ho, P.; Dodabalapur, A.; Katz, H. E.; Rogers, J. A. *Proc. Natl. Acad. Sci.* **2002**, *99*, 10252.
- (10) Pelle, M. T.; Crawford, G. H.; James, W. D. *J. Am. Acad. Dermatol.* **2004**, *51*, 499–512.
- (11) Burgess, I. F.; Lee, P. N.; Brown, C. M. *Pharm. J.* **2008**, *280*, 371–375.
- (12) Gertz, C.; Klostermann, S.; Kochhar, S. P.; Hagen, C. U. *Ol. Corps Gras, Lipides* **2003**, *10*, 297–303.
- (13) Meuwly, R.; Sager, F.; Brunner, K.; Dudler, V. *Dtsch. Lebensm.-Rundsch.* **2007**, *103*, 561–568.
- (14) Hollahan, J. R.; Carlson, G. L. *J. Appl. Polym. Sci.* **1970**, *14*, 2499–2508.
- (15) Efimenko, K.; Wallace, W. E.; Genzer, J. *J. Colloid Interface Sci.* **2002**, *254*, 306–315.
- (16) Oláh, A.; Hillborg, H.; Vancso, G. J. *Appl. Surf. Sci.* **2005**, *239*, 410–423.
- (17) Hillborg, H.; Sandelin, M.; Gedde, U. W. *Polymer* **2001**, *42*, 7349–7362.
- (18) Waddell, E. A.; Shreeves, S.; Carrell, H.; Perry, C.; Reid, B. A.; McKee, J. *Appl. Surf. Sci.* **2008**, *254*, 5314–5318.
- (19) Song, J.; Duval, J. F. L.; Stuart, M. A. C.; Hillborg, H.; Gunst, U.; Arlinghaus, H. F.; Vancso, G. J. *Langmuir* **2007**, *23*, 5430–5438.
- (20) Hillborg, H.; Tomczak, N.; Oláh, A.; Schönherr, H.; Vancso, G. J. *Langmuir* **2004**, *20*, 785–794.
- (21) Hillborg, H.; Ankner, J. F.; Gedde, U. W.; Smith, G. D.; Yasuda, H. K.; Wikström, K. *Polymer* **2000**, *41*, 6851–6863.
- (22) Hillborg, H.; Karlsson, S.; Gedde, U. *Polymer* **2001**, *42*, 8883–8889.
- (23) Kim, J.; Chaudhury, M. K.; Owen, M. J. *J. Colloid Interface Sci.* **2006**, *293*, 364–375.
- (24) Eddington, D. T.; Puccinelli, J. P.; Beebe, D. J. *Sens. Actuators, B* **2006**, *114*, 170–172.
- (25) Schneemilch, M.; Quirke, N. *J. Chem. Phys.* **2007**, *127*, 114701.
- (26) Ismail, A. E.; Grest, G. S.; Heine, D. R.; Stevens, M. J.; Tsige, M. *Macromolecules* **2009**, *42*, 3186–3194.
- (27) Shemella, P. T.; Laino, T.; Fritz, O.; Curioni, A. *J. Phys. Chem. B* **2011**, *115*, 2831–2835.
- (28) Shemella, P. T.; Laino, T.; Fritz, O.; Curioni, A. *J. Phys. Chem. B* **2011**, *115*, 13508–13512.
- (29) Efimenko, K.; Crowe, J. A.; Manias, E.; Schwark, D. W.; Fischer, D. A.; Genzer, J. *Polymer* **2005**, *46*, 9329–9341.
- (30) Smith, J. S.; Borodin, O.; Smith, G. D. *J. Phys. Chem. B* **2004**, *108*, 20340–20350.
- (31) Maple, J. R.; Hwang, M. J.; Stockfisch, T. P.; Dinur, U.; Waldman, M.; Ewig, C. S.; Hagler, A. T. *J. Comput. Chem.* **1994**, *15*, 162–182.
- (32) Hwang, M. J.; Stockfisch, T. P.; Hagler, A. T. *J. Am. Chem. Soc.* **1994**, *116*, 2515–2525.
- (33) Sides, S. W.; Curro, J.; Grest, G. S.; Stevens, M. J.; Soddemann, T.; Habenschuss, A.; Londono, J. D. *Macromolecules* **2002**, *35*, 6455–6465.
- (34) Habenschuss, A.; Tsige, M.; Curro, J. G.; Grest, G. S.; Nath, S. K. *Macromolecules* **2007**, *40*, 7036–7043.
- (35) Ryckaert, J. P.; Cicciotti, G.; Berendsen, H. J. C. *J. Comput. Phys.* **1977**, *23*, 327–341.
- (36) Plimpton, S. J. *Comput. Phys.* **1995**, *117*, 1–19.
- (37) <http://lammps.sandia.gov>; accessed 23 June 2011.
- (38) IBM and Blue Gene are trademarks of International Business Machines Corporation, registered in many jurisdictions worldwide.
- Other product and service names might be trademarks of IBM or other companies.
- (39) Aqvist, J. *J. Phys. Chem.* **1990**, *94*, 8021–8024.
- (40) Jorgensen, W. L.; Chandrasekhar, J.; Madura, J. D.; Impey, R. W.; Klein, M. L. *J. Chem. Phys.* **1983**, *79*, 926.
- (41) Werder, T.; Walther, J. H.; Jaffe, R. L.; Halicioglu, T.; Koumoutsakos, P. *J. Phys. Chem. B* **2003**, *107*, 1345–1352.
- (42) De Ruijter, M. J.; Blake, T. D.; De Coninck, J. *Langmuir* **1999**, *15*, 7836–7847.
- (43) Tsige, M.; Grest, G. S. *J. Phys. Chem. C* **2008**, *112*, 5029–5035.
- (44) Chen, C.; Wang, J.; Chen, Z. *Langmuir* **2004**, *20*, 10186–10193.
- (45) ABB internal communication.